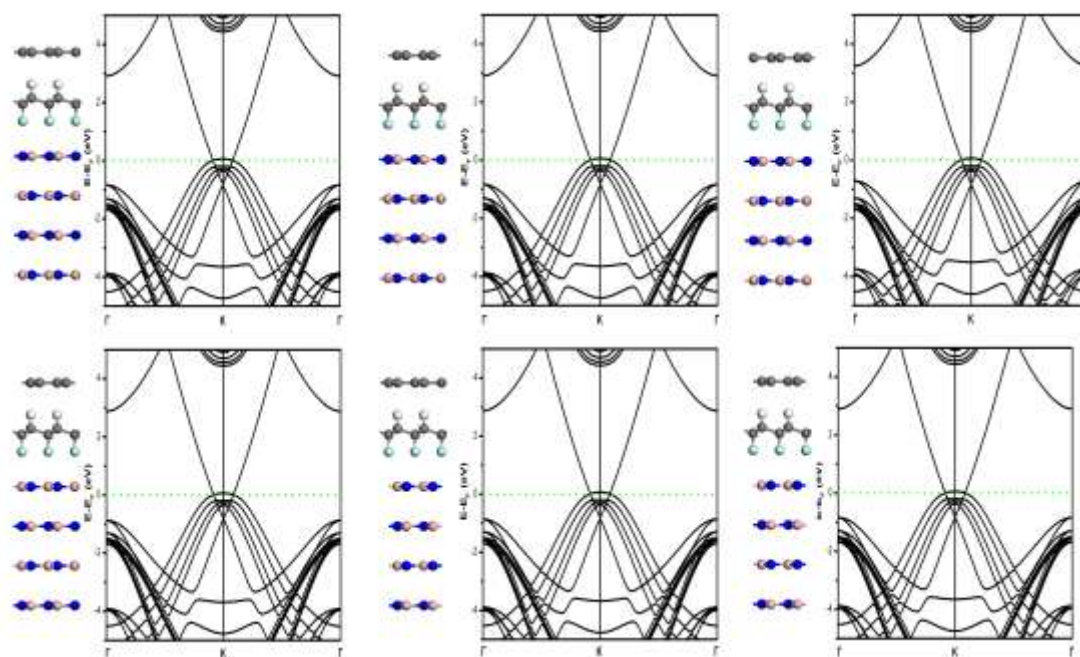


## Utilisation of Janus Material for Controllable Formation of Graphene p-n Junctions and Superlattices

Xian. Fei. Chen, Yong. Fu. Zhu,<sup>\*</sup> Qing. Jiang<sup>\*</sup>

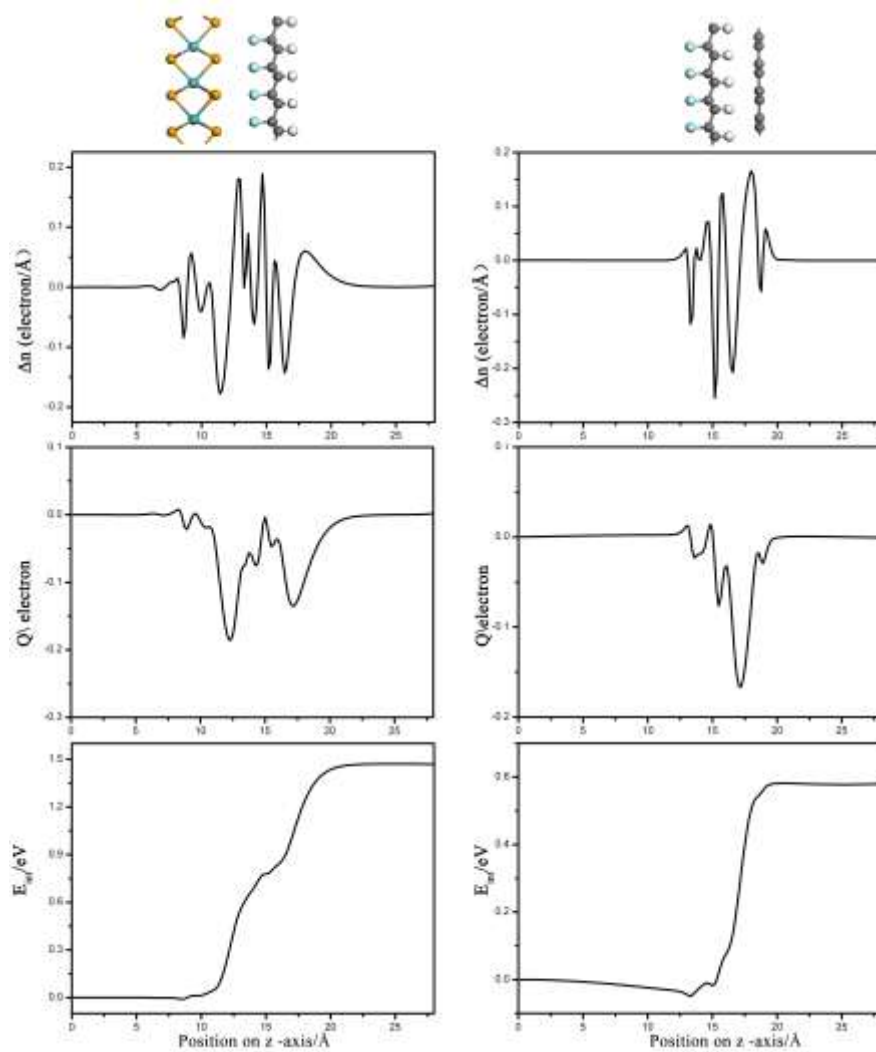
Figure S1 Atomic structures and calculated band structures of other configurations of BN/F-G-H/Graphene. The Fermi levels are set to zero as indicated by the green dot lines.

We can found that the Fermi levels shift upward, representing a p-type doping in graphene and closer examination demonstrates that the doping concentration in graphene shows little relationship with the relative disposition of graphene, buffer layer, and BN substrate.



<sup>\*</sup> Corresponding author. Tel/Fax: 86-431-85095876. E-mail address: [yfzhu@jlu.edu.cn](mailto:yfzhu@jlu.edu.cn), [jiangq@jlu.edu.cn](mailto:jiangq@jlu.edu.cn)

Figure S2 Charge rearrangements upon inserting H-G-F,  $\Delta\rho(z)$ , net charge transfer,  $Q$ , as well as the resulting change in electrostatic energy,  $E_{int}$ , for MoSe<sub>2</sub>/F-G-H, F-G-H/Graphene, BN/F-G-H and F-G-H/Graphene.



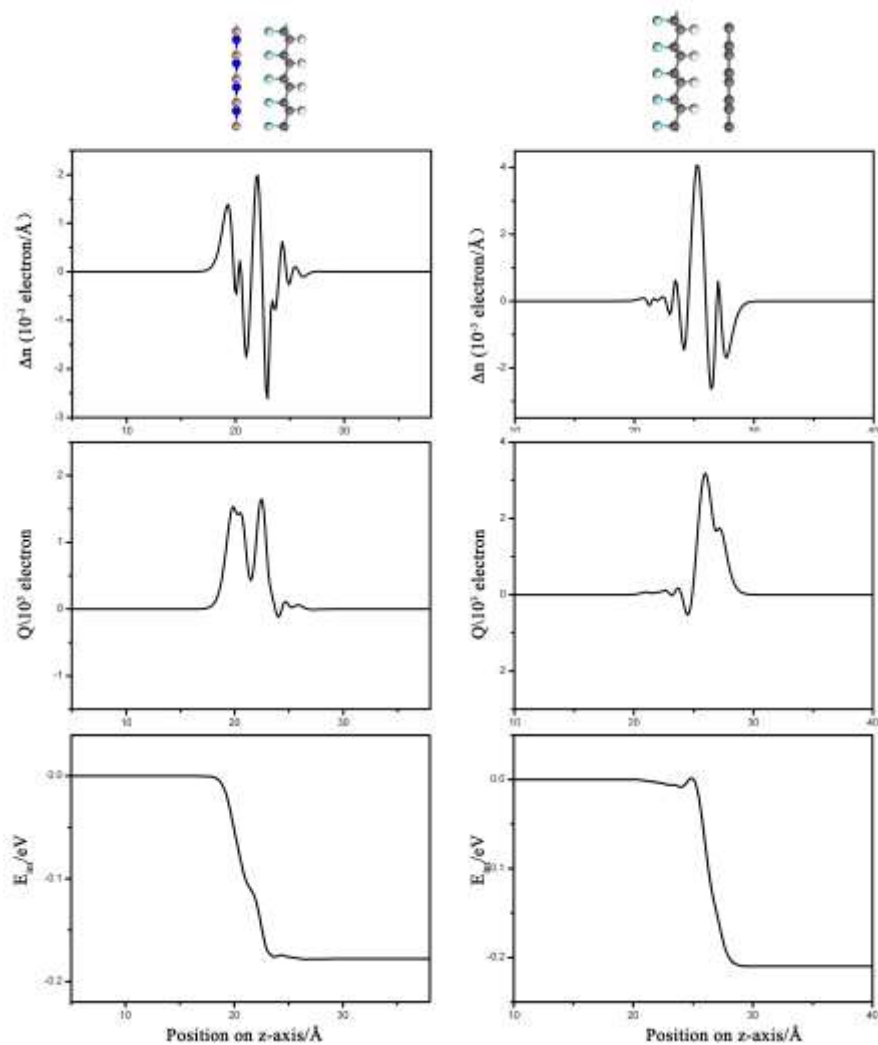


Figure S3 (a) Work function,  $W_{\text{BN}}$ , of the 4-ML BN and that for graphene  $W_{\text{G}}$  (e). Interface dipole layer induced potential energy steps between BN and F-G-F denoted as  $\Delta E_{\text{BN/F-G-H}}$  (b) and that between F-G-H and graphene layer denoted as  $\Delta E_{\text{F-G-H/graphene}}$  (d). (c) Potential energy step,  $\Delta E_{\text{vac}}$ , across the F-G-H layer. (f) The plane-averaged electron potential energy of the combined system.

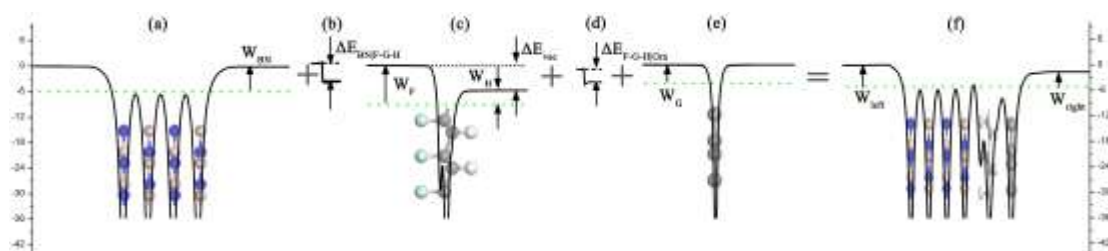


Figure S4 Optimized atomic structures and corresponding band structure of BN|H-G-F|Graphene. The bands derived from graphene and H-G-F layers are highlighted via pink and green curves, respectively.

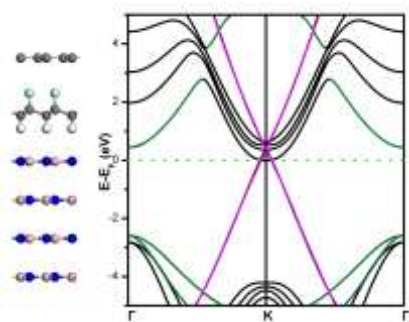


Figure S5 Dependence of the graphene Dirac point relative to the system Fermi level plotted as a function of an external field for both BN/F-G-H/Graphene and BN/H-G-F/Graphene. The Fermi level is set to zero in all plots.

